Deuteron spin–lattice relaxation in the presence of an activation energy distribution: Application to methanols in zeolite NaX

G. Stoch[a], E.E. Ylinen[b*], A. Birczynski[a], Z.T. Lalowicz[a], K. Góra-Marek[c], M. Punkkinen[b]

[a]H. Niewodniczanski Institute of Nuclear Physics of PAN, ul. Radzikowskiego 152, 31-342 Krakow, Poland

[b]Wihuri Physical Laboratory, Department of Physics and Astronomy, University of Turku, FI-20014 Turku, Finland

[c]Faculty of Chemistry, Jagellonian University, 30-060 Krakow, Poland

*Corresponding author
Dr. Eero Ylinen
Wihuri Physical Laboratory, Department of Physics and Astronomy
University of Turku, FI-20014 Turku, Finland
E-mail address: Eero.Ylinen@utu.fi

Abstract

A new method is introduced for analysing deuteron spin–lattice relaxation in molecular systems with a broad distribution of activation energies and correlation times. In such samples the magnetization recovery is strongly non-exponential but can be fitted quite accurately by three exponentials. The considered system may consist of molecular groups with different mobility. For each group a Gaussian distribution of the activation energy is introduced. By assuming for every subsystem three parameters: the mean activation energy E_0, the distribution width σ and the pre-exponential factor τ_0 for the Arrhenius equation defining the correlation time, the relaxation rate is calculated for every part of the distribution. Experiment–based limiting values allow the grouping of the rates into three classes. For each class the relaxation rate and weight is calculated and compared with experiment. The parameters E_0, σ and τ_0 are determined iteratively by repeating the whole cycle many times. The temperature dependence of the deuteron relaxation was observed in three samples containing CD_3OH (200% and 100% loading) and CD_3OD (200 %) in NaX zeolite and analysed by the described method between 20 K and 170 K. The obtained parameters, equal for all the three samples, characterize the methyl and hydroxyl mobilities of the methanol molecules at two different locations.

Key words: NMR relaxation; deuteron relaxation; methanol in zeolite; activation energy distribution; non-exponential relaxation

1. Introduction

Industrial use of zeolites as catalysts has inspired an enormous number of studies on their properties. Usage of guest molecules and investigation of their adsorption at molecular level is one of the ways to characterize zeolites. Guest–host interactions have important implications and stimulate investigation in this field [1]. A recent review by Buntkovsky et al. [2] provides an excellent introduction to the subject of mesoporous silica materials as studied by several methods.

One guest molecule of great interest is methanol. Its adsorption in NaX zeolite at low temperatures was studied experimentally by inelastic neutron scattering [3]. Molecular dynamics methods were applied to study the diffusion of methanol in faujasites [4, 5]. Quantum chemistry and DFT methods were used to study conditions affecting the adsorption of methanol in faujasites [6, 7]. In addition many different experimental methods have been used to study quest molecules including various neutron and X-ray diffraction, diffusion, optical, infrared and NMR techniques. The most often used NMR methods are the line-shape analysis of ^{2}H and ^{15}N NMR spectra, MAS NMR and NMR diffusion experiments [2]. Information has been obtained about structural features and mobilities of the framework and of various guest atoms and molecules.

To some extent the analysis of the experimental data has been complicated by the fact that although the position of the molecule in zeolite may be known, its surroundings is not known in detail. In a recent work on the mobility of methanol–d_4 in NaX the high temperature deuteron relaxation and deuteron spectra down to low temperatures were studied [8]. It was observed that to explain experimental results on spectra and relaxation in detail motional activation energies have to show reasonably broad distributions. These distributions originate from random distribution of the framework aluminium atoms and from differences in the surroundings of the guest molecules and their binding energies. Therefore e.g. the NMR spectral shape may be observed to change over a wide temperature range. Consequently, the determination of the activation energy requires special approaches. Such methods have been presented for spectral analysis [9–11].

However, there are not many methods for analysing spin–lattice relaxation under similar conditions. The so-called stretched exponent method using $\exp[-(t/\tau)^{\beta}]$, with τ and β as parameters, describes most likely the magnetization recovery quite well. Unfortunately, it is not known how the dynamic parameters like the activation energy and correlation time depend on τ and β. Cereghetti et al. [10] showed that the distribution of the activation energies can explain very well the nonexponential relaxation and lead to numerical values for the distribution width and correlation times. However, even their method has its limitations, in the presented form it is not applicable to samples, where for example two CD_3 groups are clearly at nonequivalent positions. In such a case the description of the activation energies requires two distributions centered about two different mean activation energies. Since our samples contain, in addition to methyl groups at two clearly nonequivalent positions, also hydroxyl groups at two nonequivalent positions, we have to resort to a different method.

Our approach can be used for analysing deuteron spin–lattice relaxation in the presence of several clearly nonequivalent molecular groups, each having their own activation energy distribution. For that end we must be able to describe the

magnetization recovery quite accurately. This can be done by fitting a number of exponentials, with adjustable weights and decay rates, to the experimental points. Under quite general conditions three exponentials lead to a sufficient accuracy, although the use of four or even five exponentials is possible. The obtained weights and decay rates serve as characteristic quantities, which can be calculated by introducing a Gaussian distribution for the activation energy of each molecular group with the mean activation energy E_0 and distribution width σ. When the corresponding pre-exponential factor τ_0 is defined, the Arrhenius equation yields the motional correlation time, and then the relaxation rate for a certain part of the distribution can be calculated. Such individual rates are classified into three classes by using as separating quantities the experiment–based values $(R_f R_m)^{1/2}$ and $(R_m R_s)^{1/2}$, where for example R_f is the experimentally observed relaxation rate of the fast decaying exponential. For each class we can calculate the initial relaxation rate and the corresponding weight. These are compared with corresponding experimental data leading, after several steps of adjusting the parameters E_0, σ and τ_0, to an optimal fit and the estimate of these motional parameters.

It is important to realise that although the described method is meant for analysing relaxation data, the obtained motional parameters can also be used to describe the temperature dependence of spectra.

We start the theoretical part by describing the distribution, the calculation of the relaxation rate for a certain part of the distribution, the choice of the limiting values used in separating the rates into three classes, and the calculation of the initial relaxation rate and relative weight for each class. The method is then extended to samples which contain many different molecular groups. After a short description of the samples and experimental methods, the experimental results are shown for our three samples of NaX(1.3) zeolite containing different amounts of CD_3OD and CD_3OH molecules. Calculated results are compared with the experimental data and the relation of the obtained motional parameters to various molecular groups is discussed. Finally in Conclusion some features are discussed, which were not included in the simulations but which can be taken into account in future studies.

2. Calculation of the relaxation rate

2.1. One molecular group, for example CD_3

All the methyl groups are assumed to be bonded similarly but small differences in the surroundings cause changes for example in the activation energy leading to a distribution. Let us assume the mean activation energy E_0 around which the possible activation energies $E_k = E_0 + \Delta E_k$ are distributed. Each E_k has the probability (or weight) w_k, which is obtained from the Gaussian distribution

$$w_k = C \exp(-\Delta E_k^2/2\sigma^2) \qquad (1)$$

where σ is the distribution width. In the calculations we used the values $\Delta E_k = k\sigma/20$, $k = 0, \pm1, \pm2, \ldots, \pm60$. When all the 121 different w_k values are summed up, the result must be 1. Thus $C = 1/\sum_k \exp(-\Delta E_k^2/2\sigma^2)$. Then we calculate the correlation times

$$\tau_k = \tau_0 \exp[(E_0 + \Delta E_k)/RT] \qquad (2)$$

and the corresponding relaxation rates (for a polycrystalline sample)

$$R_k = A[J(\tau_k, \omega_0) + 4J(\tau_k, 2\omega_0)] \quad (3)$$

where the spectral density functions are defined by $J(\tau_k, \omega) = \tau_k/[1+\omega^2\tau_k^2]$. The multiplier A depends on the relaxation model. For CD_3, reorienting about its threefold axis, it equals $\omega_Q^2/15$ [12, 13], where $\omega_Q = e^2qQ/\hbar = 2\pi\nu_Q$. This efficiency factor is consistent with the fact that rotation about the methyl axis leaves a part of the quadrupole interaction time independent. In the 120° rotations of this motion the C–D bonds jump between tetrahedral directions, which make the angle 109.5° with each other and also with the methyl axis. In our calculations we used the value $A = \omega_Q^2/15$. This is slightly smaller than $A = 3\omega_Q^2/40$ representing isotropic motion, which makes the quadrupole interaction completely time dependent.

Finally the total relaxation rate, in the rather rare case of *fast spin diffusion*, is obtained by adding all the R_k values

$$R = \Sigma_k\, w_k\, R_k = \Sigma_k\, w_k\, A[J(\tau_k, \omega_0) + 4J(\tau_k, 2\omega_0)] \,/\, \Sigma_k\, w_k \quad (4)$$

Spin diffusion between deuterons in solids at low temperatures is often slower than the individual rates R_k, therefore the relaxation appears nonexponential and the weighted result (4) fails to describe the magnetization recovery for longer times. In any case Eq. (4) represents the initial relaxation rate R_i. This can be compared with the experimentally observed initial relaxation rate.

The part of the quadrupole interaction, which remains time–independent under the rotation about the methyl axis, becomes at least partially time–dependent due to a motion of the methyl axis. Let the correlation times describing the axis jumping and reorientation about the axis be τ_k' and τ_k, respectively. If $\tau_k' >> \tau_k$ and the axis jumps between two tetrahedral orientations, then the additional relaxation rate is obtained from Eqs. (3, 4) when $A = \omega_Q^2/180$ and τ_k replaced by τ_k'. If the additional motion makes the remaining quadrupole interaction totally time–dependent, then $A = \omega_Q^2/120$.

When the mobility of the hydroxyl deuteron is considered, it might happen that the O–D vector does not jump between tetrahedral orientations but by smaller angles. If the possible orientations (at least three of them) lie on a cone making the angle Δ with the cone axis, the relaxation rate for randomly oriented OD groups is again obtained from Eqs. (3, 4) when the corresponding correlation time τ_j is used and A replaced by [13, 14]

$$A = (\omega_Q^2/160)(36 \sin^2\Delta \cos^2\Delta + 9 \sin^4\Delta) \quad (5)$$

2.2. Use of many exponentials

In practice nonexponential relaxation is often described by a sum of two or three exponentials with different time constants and relative weights. In the present study the magnetization recovery will be approximated by three exponentials. This procedure can be supported by the following reasoning. When the nonexponentiality is very pronounced, then even two exponentials do not lead to a satisfactory

description. Actually there is in principle no upper limit for the number of exponentials. Especially, if the span of the relaxation rates (3) of individual magnetizations representing different k values of the distribution extends over many orders of magnitude, the need for more than three exponentials may grow. On the other hand in practice four exponentials may be too many because then small errors of experimental points lead easily to large scatter in the values of individual rates and weights, which makes subsequent consideration of the obtained results difficult and prevents strict conclusions. Therefore we chose to use three exponentials to simulate the observed data.

To our knowledge there exists no model yet which could compare the experimental time constants (or the corresponding relaxation rates, which are inverses of the time constants) with a detailed theory in such a complicated case. To make use of the described model we have to select by some method from the individual rates (3) those which contribute to each one of the three experimentally observed components. For this purpose we have not found any theoretical principle but consider the use of the geometric mean of the experimentally observed relaxation rates as a good choice. When the rates of the fast, medium and slow components are called R_f, R_m and R_s, respectively, the limiting values are $L_{fm} = (R_f R_m)^{1/2}$ and $L_{ms} = (R_m R_s)^{1/2}$. These values are first calculated from experimental rates for each temperature and then continuous curves are worked out, which fit them as closely as possible.

When we simulate for example the experimentally observed medium component by this method, we select from the individual relaxation rates only those, which obey the relation $L_{fm} > R_{k'} > L_{ms}$ (for these selected k values we use k'), sum then up the weighted rates $w_{k'}R_{k'}$, and finally divide this sum by $\Sigma_{k'} w_{k'}$ to calculate the corresponding initial relaxation rate R_{im} (the weights w_k of the excluded rates are taken equal to zero).

2.3. Several nonequivalent groups

The sample may contain methyl and OD groups, which are differently bonded (for example CD_3OD in NaX). Then we have to assume for each nonequivalent group its own mean activation energy E_0, the distribution width σ and the pre-exponential factor τ_0. Furthermore, we have to introduce an additional weight w_a, which depends on deuteron abundance. If CD_3OD molecules appear, with equal abundance, in two essentially nonequivalent sites in the sample, then the abundance–dependent weights w_a are 3/8, 3/8, 1/8 and 1/8 for the nonequivalent methyl and OD groups, respectively. The weight w_k in Eq. (4) has then to be replaced by the product $w_k w_a$. In addition, a similar summation as that over k in Eq. (4) has to be worked out for all the four nonequivalent groups in order to obtain the initial relaxation rates. The selection of the individual relaxation rates into three categories is done by comparing them to the limiting values L_{fm} and L_{ms}.

There are essentially two different methanol positions; those called I or horizontal are near the Na atoms and those in the positions II (called also vertical), which are hydrogen bonded via the hydroxyl deuteron to the oxygens of the zeolite framework [15]. It is reasonable to assume that both the positions I and II are equally occupied in CD_3OH–NaX (200%), which makes w_a values equal to ½. Although in CD_3OH–NaX (100%) the positions II can be shown to be preferred, the experiments show that they

are not exclusively occupied. We therefore take the abundance–dependent occupancy w_a of the positions I as another parameter, which means that the corresponding occupancy for the positions II is $1 - w_a$.

In Fig. 1 we show the deuteron magnetization recovery in CD_3OH–NaX (100%) after saturation at 30 K by using three different linear time scales. The solid curve is a three–exponential least–squares fit to the experimental data, corresponding to the relaxation rates $R_f = 174\ s^{-1}$, $R_m = 17.5\ s^{-1}$ and $R_s = 1.18\ s^{-1}$ and the respective weights 0.470, 0.335 and 0.195. The standard deviation for the rates is $9\ s^{-1}$, $1.5\ s^{-1}$ and $0.10\ s^{-1}$, respectively, while that for the weights is 0.022. The curve is seen to follow the experimental data very closely. The relaxation rates define the three different time scales. The dashed curve is the three–exponential curve with the initial relaxation rates $R_{fi} = 191\ s^{-1}$, $R_{mi} = 23.5\ s^{-1}$ and $R_{si} = 2.00\ s^{-1}$ and practically the same weights. These rates and weights are based on the parameters of Table I, which were obtained by simulating the temperature dependence of the experimental relaxation rates and relative weights by the method described briefly above (to be described later on in more detail). It goes slightly higher than the experimental points showing that the calculated relaxation rates in Fig. 7 are slightly above the observed values at 30 K. The dotted curve is a really multiexponential curve, which was obtained from the data of Table I by calculating separately each partially recovered magnetization, corresponding to all the different values k of the activation energy distribution, as the function of the recovery time t and adding together these magnetizations (without any selection into three components). In principle this curve should give the best description of the experimental points and it really fits the experiment very well. When this curve is fitted with three exponentials, the following relaxation rates are obtained $R_{fn} = 171\ s^{-1}$, $R_{mn} = 15.6\ s^{-1}$ and $R_{sn} = 0.913\ s^{-1}$ where the second subindex is used to distinguish these rates from the experimental ones. These rates should be nearer to the experimental rates than the calculated initial rates. Unfortunately the rates R_{fn}, R_{mn} and R_{sn} are much more difficult to calculate than the corresponding initial rates.

In principle the initial rates are expected to be somewhat larger than the experimental rates because in the case of nonexponential relaxation the initial rate is always larger than the rate at any later time. This argument is consistent for example with the ratio $R_{fi}/R_f = 1.10$. More reliable values for the ratio can be obtained by comparing the initial rates with those calculated from the multiexponential behaviour (dotted curve), since they are all based on the parameters of Table I. The results are $R_{fi}/R_{fn} = 1.12$, $R_{mi}/R_{mn} = 1.50$ and $R_{si}/R_{sn} = 2.19$. The fact that the ratios are larger than 1 probably causes some error, but it is not expected to cause significant error in the activation energies, which depend more on the temperature dependence than on the exact numerical values of the observed and calculated rates. It seems possible that this error can be corrected in future by dividing the calculated initial rate by the relevant ratio (for example R_{fi}/R_{fn}) before comparing with the experimental relaxation rate.

3. Experimental

Zeolite NaX(1.3) (supplied by Sigma–Aldrich) was activated *in situ* in an NMR sample tube. The sample was first evacuated at room temperature for 30 minutes, and then the temperature was raised, at the rate of 5 K/min, to 700 K and kept there in vacuum for 1 h. The doses of CD_3OD and CD_3OH were sorbed into the zeolite up to

100% and 200% of the total coverage of Na^+ ions. The doses were determined by controlling the methanol pressure to the accuracy of 100 Pa. The use of the standard preparation method, as described for example in [16], removes effectively any possible water. All the samples were sealed in 24 mm long glass tubes with the outside diameter 5 mm. We use for our NaX samples the following labels: Sample 1 contains 200% of CD_3OH, Sample 2 200% of CD_3OD, and Sample 3 contains 100% of CD_3OH.

The experiments were carried out at the deuteron resonance frequency 46 MHz with TECMAG Apollo spectrometer. The technical details are explained elsewhere [8].

Spin–lattice relaxation below 170 K was studied by first saturating the deuteron magnetization by a sequence of $\pi/2$ resonant pulses and observing then, after a variable time t, the partially recovered magnetization by the quadrupole echo [8]. The echo amplitude at maximum was taken proportional to the total deuteron magnetization. Above 170 K most measurements were done by observing the free induction signal and taking the total magnetization proportional to the integrated signal area over a certain time range after the dead time. The magnetization recovery was described by fitting, by the least–squares method, the function $M_Z(t) = \Sigma_{i=1-3} M_i [1 - \exp(-R_i t)] + c_0$ to the experimental points. The small parameter c_0 takes into account that the saturation may not be perfect. The fitting procedure gives the three relaxation rates and magnetization amplitudes M_i, from which the relative weights are obtained as for example $w_1 = M_1/(M_1 + M_2 + M_3)$.

4. Comparison with experiment and discussion

4.1. CD_3OH–NaX (200 %)

We start with this sample since it contains no hydroxyl deuterons and its methanol groups can be assumed to occupy only two positions I and II. The experimentally observed recovery of the deuteron magnetization was fitted with a sum of three exponentials at each temperature for $T < 140$ K. The corresponding relaxation rates and weights are shown in Figs. 2 and 3, respectively. They were obtained by quadrupole echo measurements, only two points for $T > 220$ K were determined from FID. All the three rates vary smoothly with temperature; below 140 K they at first grow when T is lowered, then show a broad maximum and finally start to decrease slowly below 40 K. The relative weights show stronger variation with temperature. It is worth noticing that the extracted components are not in a one-to-one correspondence with either CD_3(I)'s or CD_3(II)'s, otherwise only two components could be extracted. This means that the distributions of the activation energies and correlation times are rather wide. Above 140 K the nonexponentiality of relaxation decreases and for $T > 150$ K the magnetization recovery is exponential. The transition to exponential relaxation occurs about 25 K below the temperature $T_S = 169.5$ K, above which the deuteron spectrum of Sample 2 was observed to show an intense narrow line [8]. At T_S the methanols at positions I become free to move. Above T_S the relaxation is clearly exponential.

To simulate these results with our model we assume that the surroundings of both the positions I and II have a statistical nature and, therefore, the activation energies of the CD_3 groups are distributed around the two mean activation energies E_0 within the range described by the corresponding distribution widths σ. For the calculation of the

correlation times we need to define the pre-exponential factors τ_0. Thus there are altogether six parameters. The abundance–dependent weight for both positions is ½. The deuteron quadrupole frequency of all the CD_3 groups was taken equal ν_Q =160 kHz. In order to make the individual rates (3) (corresponding to the 121 different k values) contribute to the relaxation rate of the selected component, we calculated the limiting values L_{fm} and L_{ms} and fitted them with suitable mathematical functions (cf. Fig. 2). Then we gave starting values for the mentioned six parameters and calculated the initial relaxation rates R_{fi}, R_{mi} and R_{si} and the relative weights w_f, w_m and w_s as a function of temperature for 20 K < T < 140 K. The parameter values were changed and new rates and weights were calculated. In the later stages of the refinement we simulated, at each change of the parameters, also the relaxation results for Samples 2 and 3 and the temperature–dependent amplitude of the rigid doublet in the spectrum of Sample 2. Finally we ended up with the initial relaxation rates and weights shown in Figs. 2 and 3 for Sample 1. The corresponding parameter values are given in Table I. (If we were considering only this sample, the best–fit parameters would be somewhat different. Especially the activation energy of the methyls I would be somewhat reduced. However, we use the same parameters for all three samples and therefore had to make compromises.) Nevertheless, the agreement between the experimental and simulated rates and weights is quite satisfactory.

As mentioned above, the relaxation becomes exponential above 150 K. The exponentiality requires always some kind of spin diffusion, which is faster than the relaxation rate. In our samples the normal spin diffusion via the magnetic dipolar interaction between the deuterons of neighbouring methyl groups is nearly nonexistent. However, a mechanism equivalent to spin diffusion can be found in the motion of methanols. Above T_S the methanols near the positions I are no more strictly localized but start to move. Above 140 K the corresponding frequency is probably larger than $1/T_1$ and in such a case methyl groups can experience many different activation energies and correspondingly different relaxation rates during the recovery towards equilibrium, leading to an averaging of the observed relaxation rate. Thus no selection of the individual relaxation rates is needed, instead we can compare the initial relaxation rate (4) with experiment. A short piece of a curve, representing the initial relaxation rate as calculated from the parameters of Table I, is shown in Fig. 2. It agrees rather well with the few experimental points between 150 K and 170 K but deviates clearly from experiment above T_S, showing that a different process starts to dominate the relaxation [8].

In our previous study the faster reorienting methyl groups were concluded to belong to the methanols in the positions II by considering the bonding of methanols in the two positions [8]. These methanols are hydrogen–bonded via the hydroxyl hydrogen to a framework oxygen of the zeolite. Experimental results on the temperature dependence of the translation–to–reorientation transition, observable for example in the deuteron relaxation of methanols in zeolites at higher temperatures, show that the positions II are also preferably occupied by methanols. This preferential occupation is also supported by the experimental deuteron spectra of NaX with the 100 % content of CD_3OH or CD_3OD, which show a more intense motionally narrowed component than the corresponding 200 % samples.

The mean activation energy 2.7 kJ/mol for the methyl groups of methanols in the positions II (later on called methyl groups II) means that these methyls are undergoing 120^o rotational jumps at a rate which exceeds the deuteron quadrupole coupling near and above 20 K. The corresponding tunnelling frequency is of the magnitude 200–300 MHz below 20 K and in such a case one might expect tunnelling sidebands

in the deuteron spectrum [17, 18]. The sidebands were not observed, which provides another proof for fast motion, because the sidebands can be observed only in the presence of methyl rotation slower than the doublet splitting.

In simulations we used always Eq. (4) with $A = \omega_Q^2/15$, which includes only the effect of the of 120^o rotations about the methyl axis. Some earlier results on deuteron spectrum suggest that a part of the faster reorienting methyl groups are moving more freely so that also the methyl axis is changing direction. Such a motion would open a new relaxation channel with the maximum efficiency $A = \omega_Q^2/120$. But because of this rather small efficiency and the necessity to introduce three additional motional parameters into simulations, this relaxation channel was ignored.

The faster reorienting methyl groups dominate the relaxation rate of the fast component below 50 K and contribute also to other components with variable weight, for example they dominate the medium component practically in the entire temperature range of the experiments.

The mean activation energy of the more slowly reorienting CD_3's, 6.4 kJ/mole, is so large that these methyls give rise to a rigid doublet in the spectrum at low temperatures. Their contribution to the relaxation rate of the fast component reaches maximum near 70 K. Thus with rising temperature they can be expected to exhibit the rotation–narrowed doublet with an increasing weight (with the doublet separation reduced to 1/3 of the rigid–spectrum value) at temperatures roughly above 40 K, in a good agreement with the experimental spectra for Sample 2 (Fig. 6).

4.2. CD_3OD–NaX (200 %)

This sample is discussed next because it is very similar to the previous one, only the hydroxyl protons are replaced by deuterons. The experimental data were obtained by the quadrupole echo below 170 K and by FID above it. The recovery of its deuteron magnetization was analysed by a sum of three exponentials with adjustable relaxation rates and relative weights. The results are shown in Figs.4 and 5. In principle the relaxation rates below 140 K behave in the same way as those of Sample 1, but the temperature dependence of the rates of the medium and slow components is stronger now. Another difference is the much smaller values for the rates of the medium and slow components. Also the temperature dependence of the weights departs from those in Figs.3. Still another difference is the fact that three exponentials are required to describe the nonexponential magnetization recovery between 140 K and 170 K. Even at temperatures few degrees above T_S some methanols remain localized so that three–exponential relaxation is still observed, most likely due to a distribution of the binding strength. Nevertheless, at still higher temperatures the relaxation, as measured from the amplitude of the free induction signal, becomes biexponential as reported already in [8] and also shown in Fig.4. The lower rates are believed to describe methyl deuterons and the higher rates the hydroxyl deuterons. The lower curve agrees reasonably with the rates of Sample 1 just above T_S but starts to deviate from them at higher temperatures.

To make the individual magnetizations contribute to the right component, the limiting values L_{fm} and L_{ms} were calculated and fitted with mathematical functions (Fig. 4). For the motional parameters of the methyl groups I and II we use the same values of Table I, which were already used to describe the CD_3OH–NaX (200 %) data.

For the OD deuterons we have not yet defined any motional parameters. The deuteron spectra of Sample 2 were first interpreted to be consistent with the quadrupole frequency ν_Q = 205 kHz at 20 K. Above 50 K the OD(I) deuterons start to contribute to the motionally narrowed doublet, with the doublet splitting roughly one third of that of the rigid doublet, the quadrupole frequency being 150 kHz [8]. In the simulations we used $\nu_Q = \omega_Q/2\pi$ = 205 kHz, although newer experiments for example on CD_3OD–NaX (100 %) suggest that ν_Q could be somewhat smaller. Simulated curves for smaller ν_Q would probably be somewhat modified, still recalculations were not considered necessary.

The described behaviour needs two different motions, limited jumps to reduce ν_Q from 205 kHz to 150 kHz below 50 K and a reorientation of the O–D vector similar to that of a C–D vector in methyl reorientations about the methyl axis above 50 K. The former motion is qualitatively equivalent to a motion of the O–D vector on a cone as described above. The corresponding relaxation rate for the fraction k of the activation energy distribution is obtained from Eqs. (3) and (5)

$$R_k(\mathrm{lj}) = \mathrm{E}\, w_k\, (\omega_Q^2/15)[J(\tau_{lj}, \omega_0) + 4J(\tau_{lj}, 2\omega_0)] / \Sigma_k\, w_k \qquad (6)$$

where the efficiency factor E equals $E = (3/32)(36\sin^2\Delta\cos^2\Delta + 9\sin^4\Delta)$. The correlation times τ_{lim} and τ_r, the former describing the motion on the cone and the latter methyl–like reorientations, define the combined correlation time $\tau_{lj} = \tau_{lim}\tau_r/(\tau_{lim} + \tau_r)$, which was adjusted so that the maximum of (6) appears near 56 K. We used the value E = 0.66 in the simulations, which leads to the value 29° for the angle Δ.

The motion of the O–D vector on the described cone reduces also the spectral splitting. When the effective quadrupole frequency is assumed to follow the expression $\nu_{Qeff} = (1/2)(3\cos^2\Delta - 1)\,\nu_Q$ and ν_Q is taken equal to 205 kHz, the effective frequency becomes 133 kHz. This is of the same magnitude as the observed frequency 150 kHz.

The other motion is the 120° rotations of the O–D vectors about the rotation axis, analogously to the deuteron motion in methyl groups. The resulting relaxation rate can thus be described by

$$R_k(\mathrm{rot}) = (1-\mathrm{E})\, w_k\, (\omega_Q^2/15)[J(\tau_r, \omega_0) + 4J(\tau_r, 2\omega_0)] / \Sigma_k\, w_k \qquad (7)$$

The factor 1–E = 0.34 takes into account that a major part of the total relaxation efficiency was already consumed by limited jumps and only the remaining part is available for the 120° rotations above 60 K. The correlation time τ_r was chosen so that the maximum contribution of (7) appears near 100 K, contributing there mainly to the relaxation of the fast component. Thus the total contribution of the OD(I) deuterons to the relaxation rate equals the sum of (6) and (7) $R_k(\mathrm{ODI}) = R_k(\mathrm{lj}) + R_k(\mathrm{rot})$.

The spectral area of Pake doublets in Sample 2 equals 0.625 below 20 K corresponding to the combined contributions of OD(I), OD(II) and CD_3(I). Experimental spectra show that this combined weight starts to decrease above 30 K [8]. When the parameters of Table I are used for the deuterons of OD(I) and CD_3(I), the combined weight of the Pake doublets can be calculated as a function of temperature. In Fig. 6 the continuous curve represents the spectral area of the OD(I), OD(II) and CD_3(I) contributions, integrated over the correlation time distributions for the correlation times longer than 10^{-6} s, which was taken as the condition for the line narrowing in this case. The continuous curve was calculated from the results of Table

I without any additional parameters. The combined contribution of OD(I) and OD(II) is shown by the dashed line. Above 70 K only the spectrum of OD(II) remains rigid corresponding to the Pake spectral area 0.125. The simulated results agree very well with experiment.

The deuterons OD(II) are believed to be highly hindered in the entire temperature range of our experiments. We tried two models: a) a temperature–independent relaxation rate with a distribution and b) Eq. (6) with the assumption that the jump angle Δ of the O–D vector about its equilibrium position increases with temperature from a small value towards $\Delta = 70.5^{\circ}$ (corresponding to the methyl geometry). Both the approaches a) and b) lead roughly to equally good fits with experiment. Finally the choice a) was adopted and the relaxation rates were calculated from the equation $R_k(\mathrm{ODII}) = R_0 \exp(-E_k)$ with $R_0 = 49.8\ \mathrm{s}^{-1}$. The corresponding weights were calculated from the Gaussian distribution with the mean value $E_0 = 9.62$ and the width 1.80, both dimensionless quantities. The simulated curves for the relaxation rates and weights, as functions of temperature for 20 K < T < 140 K, are shown in Figs. 4 and 5, and the corresponding parameters in Table I. The overall agreement with experimental values is rather good, largest deviations appearing in the relaxation rate of the medium component and in the low–temperature weights.

In Sample 1 an exponential relaxation was observed above 150 K. Because in Sample 2 the relaxation is biexponential above 170 K, one would analogously expect a biexponential relaxation soon above 150 K in Sample 2. It is difficult to imagine that the methyl motions in CD_3OD and CD_3OH would differ essentially from each other. Therefore the appearance of three exponentials between 150 K and 170 K is probably related to the presence of hydroxyl deuterons in Sample 2, especially to those of the more strongly bonded methanols in the positions II. Actually we extrapolated the simulated curves in Figs. 4 and 5 to temperatures 140 K < T <170 K and obtained rather good fits with experiment. This shows that the same motions as below 140 K are still dominant. The fact that the experimental results for the rates of the medium and slow component and the weight of the slow component are slightly larger than the extrapolated curves just below 170 K might be an indication of another relaxation process, but it might also be caused by a small error in the extrapolated part of the limiting curves L_{fm} and L_{ms}.

In simulations we excluded such individual relaxation rates R_k (cf. Eq. (3)), which were smaller than a certain lower limit. This exclusion can be justified by the fact that experimentally such magnetizations, which relax much more slowly than the repetition rate of the experiment, are not observed at all. The limit was set to about one tenth of the relaxation rate of the slow component, which means $0.1\ \mathrm{s}^{-1}$ for the samples 1 and 3 and 10^{-4} s for the sample 2. Therefore, the weights had to be renormalized at low temperatures, which leads to somewhat different temperature dependence below 25 K in Figs. 4 and 5.

It is somewhat surprising that although we used the same motional parameters for the CD_3(I)'s and CD_3(II)'s as for the sample 1, the calculated rates for CD_3OD–NaX (200 %) are so much shifted towards lower values. Physically the slower relaxation relates to the hydroxyl deuterons, which extend the span of individual relaxation rates towards lower values and thus also the relaxation rates of the medium and slow component become smaller than in CD_3OH–NaX (200 %). Therefore the limiting values L_{fm} and L_{ms} are lowered, which causes a different selection of the individual magnetizations to the three components and consequently to the reduced calculated values of R_m and R_s.

4.3. CD_3OH–NaX (100 %)

All the experiments were carried out by observing the quadrupole echo, with the exception of the four highest–temperature points for $T > 200$ K, which were determined from the FID signal. The experimentally observed relaxation rates and corresponding weights are shown for Sample 3 in Figs. 7 and 8. They are quite similar to those of Sample 1, also above T_S. The calculated limiting values L_{fm} and L_{ms} are shown as dashed curves. The simulation of these data by our method is based on the parameters given in Table I. The only new parameter is the relative weight of the methanol molecules in positions I, w_a, and in positions II, $1- w_a$. The calculated results are shown in Figs. 7 and 8 for $20 \text{ K} < T < 140$ K. It turned out that the best fit was obtained with $w_a = 0.25$. This parameter influences strongly the temperature dependence of the weight of the fast relaxing component, shown as the topmost figure of Figs. 8. Because the obtained value is smaller than 0.5, the methanol groups should occupy preferably the positions II. This agrees reasonably well with the spectral amplitudes for CD_3OD–NaX (100 %) at low temperatures, which lead to $w_a = 0.15$.

In spite of the careful preparation of the samples as described in Experimental, there may be some uncertainty in the methanol concentration. If for example the CD_3OH content of Sample 1 were 15 % smaller than the claimed value 200 % (= twice the number of the Na^+ ions) and if the reduction would happen only in the occupation of the positions I, then w_a of Sample 1 would equal 0.41. This is not so far from the relaxation–based value $w_a = 0.25$ for Sample 3 and may account at least partly for the similarity of the experimental data for Samples 1 and 3.

To explain the exponential relaxation of Sample 3 between 150 K and 170 K, we calculated the initial relaxation rate according to Eq. (4) by using the parameters of Table I and $w_a = 0.25$. The results are presented in Fig. 7 by a short piece of a curve, which fits well the few experimental points for this temperature range.

In addition to bonding to the positions I and II, methanol molecules may be also bonded to other methanols by hydrogen bonds, forming for example clusters [15]. However, such bonding and clusters, especially trimers, are expected in the present samples only above $T_S = 170$ K, where the methanols near positions I are no more localized [8].

5. Conclusion

The presented method includes two approximations, (a) the totally nonexponential relaxation was described with three exponentials and (b) the calculated relaxation rates for the fast, medium and slow components are initial relaxation rates and not normal ones obtained by fitting the nonexponential relaxation of each component by one exponential. The first approximation, though not valid in principle, is practically correct because three exponentials described all our results very well. Even the second approximation should not be of major importance since the simulated curves agree quite reasonably with most experimental results for relaxation and spectra. Furthermore, we are mainly interested in the activation energies, which depend more

strongly on the temperature dependence of the observed and calculated rates than on the exact numerical values of the rates. In future it may be possible to correct the initial rates before comparison with the experimental ones.

The relaxation processes described above depend on many parameters; each of the four basically nonequivalent motions has their own central activation energy E_0, distribution width σ and the pre-exponential factor τ_0. Furthermore, we have introduced the efficiency factors 0.66 for OD(I)'s of Sample 2 and the abundance–dependent parameter w_a for Sample 3. Therefore we cannot claim that the presented curves provide the final, exact explanation. Actually comparable fits were obtained also with some other values of the parameters, but those in Table I are based on practically the smallest possible number of parameters and agree with the main features of the spectra. In addition, instead of one curve presenting the observed relaxation rates as a function of temperature (the usual case), we now have three such curves and two additional curves representing the relative weights for each of our three samples (the third weight is redundant because the sum of weights equals 1), which altogether means 15 curves. Thus, there is only about one parameter per a curve, and therefore the reached results can be considered as quite successful.

There are also some other factors which were ignored in simulations but may still be important under some conditions. In general, these features could be taken into account, but they would unavoidably add to the number of required parameters, and therefore they were ignored. For example we did not take into account the motion of the methyl group axis, which seems to be present already at 25 K in the motion of the faster reorienting methyl groups. Another simplification is the use of constant values for the activation energies. Quite often the apparent activation energies are observed to become smaller at lower temperatures and incoherent tunnelling may make the correlation time even practically temperature independent [19–21]. This is especially true for spin–lattice relaxation in carboxylic acid dimers at low temperatures [21 and references therein]. Unfortunately, the same relaxation model is not applicable in our samples. If these effects could be properly included in the model, the theoretical curves would no doubt follow experimental curves more closely, but at the expense of some additional parameters.

Still another factor is the effect of a tunnel frequency ω_t much larger than the resonance frequency ω_0. The activation energy 2.7 kJ/mol means that the tunnelling frequency of the methyl groups II is expected to become larger than ω_0 somewhere near 40 K and it increases towards 200–300 MHz when temperature is lowered. Although such a large tunnelling splitting does not affect the deuteron spectrum when the frequency of the methyl reorientation $1/\tau_c$ is much larger than the quadrupole coupling frequency ω_Q, it can alter the relaxation, at least of those CD_3's which tunnel and rotate only about the methyl axis at low temperatures. Deuteron relaxation in such a case was thoroughly discussed in [22]. The methyl groups at the E species levels relax still roughly at the rate (4), because their relaxation is dominated by such transitions, which do not change the tunnelling energy. However, the methyl groups at the A levels relax only via transitions to the E levels, which change also the tunnelling energy. Therefore, at least a part of the A level magnetization of the methyl groups II should relax at a reduced rate below 30 K, which is approximately obtained from that of the E level magnetization via multiplication by the $(\omega_0/\omega_t)^2$.

Consequently, the relaxation rates and weights of the fast and medium components can be expected to change somewhat for $\omega_t\tau_c > 1$ (roughly $T < 30$ K). Furthermore, there could appear a maximum in the relaxation rate of the medium component at $\omega_t\tau_c$

= 1, as predicted by Haupt [19] and observed for example in the proton relaxation in methylpyridines [20]. Such a maximum should be most clearly observable in the relaxation rate of the medium component of Samples 1 and 3, which do not have hydroxyl deuterons. However, the experimental points for all the components in Figs. 2 and 7 vary smoothly even through the temperature range 30–40 K. The absence of any traces of the maximum is probably a consequence of the smearing effect of the activation energy distribution. In principle the effects of a large ω_t could be included in our model, but it would require the evaluation of the tunnel splitting and its temperature dependence for each value of the activation energy. Furthermore, there is uncertainty about the correlation times τ_c as described above. Because a proper inclusion of these facts would remarkably complicate the simulations, we did not take them into account.

In spite of the mentioned deficiencies, the described method leads to a quite reasonable agreement with experimental results on relaxation and spectra. It is able to give information about motions in the presence of highly nonexponential spin–lattice relaxation, caused by wide distributions of activation energies. Together with the spectral information, it leads to estimates of the central activation energies, correlation times and distribution widths, about which there is rather little knowledge so far. Even in the present form, which uses only a minimum number of adjustable parameters, the obtained results are encouraging. Very likely some of the ignored features mentioned above will be included in simulations of the future studies.

Acknowledgements

Financial support from Jenny and Antti Wihuri Foundation is acknowledged.
This study was a part of the project generously supported by the National Science Centre, Poland, Grant No. N202 127939 during 2010-2013.

References

[1] D.F. Shantz, R.F. Lobo, Top. Catal. 9 (1999) 1–11.
[2] G. Buntkowsky, H. Breitzke, A. Adamczyk, F. Roelofs, T. Emmler, E. Gedat, B. Grünberg, Y. Xu, H-H. Limbach, I. Shenderovich, A. Vyalikh, G. Findenegg, Phys. Chem. Chem. Phys. 9 (2007) 4843–4853.
[3] R. Schenkel, A. Jentys, S.F. Parker, J.A. Lercher, J. Phys. Chem. B 108 (2004) 7902–7910.
[4] D.F. Plant, G. Maurin, R.G. Bell, J. Phys. Chem. B 111 (2007) 2836–2844.
[5] T. Nanok, S. Vasenkov, F.J. Keil, S. Fritzsche, Microporous Mesoporous Mater. 127 (2010) 176–181.
[6] D.F. Plant, G. Maurin, R.G. Bell, J. Phys. Chem. B 110 (2006) 15926–15931.
[7] J. Sielk, T. Wieland, A. Lüchow, J. Mol. Structure THEOCHEM 910 (2009) 8–13.
[8] Z.T. Lalowicz, G. Stoch, A. Birczynski, M. Punkkinen, E.E. Ylinen, M. Krzystyniak, K. Góra-Marek, J. Datka, Solid State Nucl. Magn. Reson. 45–46 (2012) 66–74.
[9] E. Rössler, M. Taupitz, K. Börner, M. Schulz, H-M. Vieth, J. Chem. Phys. 92 (1990) 5847–5855.
[10] P.M. Cereghetti, R. Kind, J.S. Higgins, J. Chem. Phys. 121 (2004) 8068–8078.
[11] J.M. Griffin, A.J. Miller, A.J. Berry, S. Wimperis, S.E.Ashbrook, Phys. Chem. Chem. Phys. 12 (2010) 2989–2998.
[12] J.C. Pratt, A. Watton, H.E. Petch, J. Chem. Phys. 73 (1980) 2542–2546.
[13] J.C. Pratt, A. Watton, J. Phys. C: Solis State Phys. 19 (1986) 5729–5744.
[14] L.P. Ingman, E. Koivula, M. Punkkinen, E.E. Ylinen, Z.T. Lalowicz, Physica B 162 (1990) 281–292.
[15] M.W. Anderson, P.J. Barrie, J. Klinowski, J. Phys. Chem. 95 (1991) 235–239.
[16] Z.T. Lalowicz, G. Stoch, A. Birczynski, M. Punkkinen, M. Krzystyniak, K. Gora-Marek, J. Datka, Solid State Nucl. Magn. Reson. 37 (2010) 91–100.
[17] Z.T. Lalowicz, U. Werner, W. Müller-Warmuth, Z. Naturforsch. 43a (1988) 219–227.
[18] A. Detken, P. Focke, H. Zimmermann, U. Haeberlen, Z. Olejniczak, Z.T. Lalowicz, Z. Naturforsch. 50a (1995) 95–116.
[19] J. Haupt, Z. Naturforsch. 26a (1971) 1578–1589.
[20] W. Müller-Warmuth, R. Schüler, M. Prager, A. Kollmar, J. Chem. Phys. 69 (1978) 2382–2392.
[21] J.L. Skinner, H.P. Trommsdorff, J. Chem. Phys. 89 (1988) 897–907.
[22] G. Diezemann, Appl. Magn. Reson. 17 (1999) 345–366.

Table I
Motional parameters for methyl and hydroxyl groups of methanol in NaX(1.3)

	CD_3(I)	CD_3(II)	OD(I) (lim. jumps)	OD(I) (rot)
E_0 (kJ/mol)	6.4	2.7	6.0	7.3
σ (kJ/mol)	1.2	0.6	0.25	0.6
τ_0 (10^{-14} s)	1.5	60	0.7	30

Figure captions

Fig.1. Recovery of the deuteron magnetization in Sample 3 after saturation vs time in three different linear time scales: (o) experimental results, (solid curve) three–exponential fit to experiment, (dashed curve) three–exponential behaviour with the initial rates and weights calculated from the values of Table I, (dotted curve) multiexponential recovery based on Table I without selection of the calculated rates (see text).

Fig. 2. Experimental relaxation rates for the fast (filled circles), medium (squares) and slow (diamonds) components of Sample 1. The calculated initial rates are represented by solid curves. The limiting values L_{fm} and L_{ms} are shown by dashed curves. Rates for the exponential relaxation are shown by open circles and fitted by Eq. (4) for 170 K > T >150 K.

Fig. 3. Experimental weights for the fast (filled circles), medium (squares) and slow (diamonds) components of Sample 1. The calculated weights are represented by solid curves.

Fig. 4. Experimental relaxation rates for the fast (filled circles), medium (squares) and slow (diamonds) components of Sample 2. The calculated initial rates are represented by solid curves. The limiting values L_{fm} and L_{ms} are shown by broken curves. The biexponential relaxation above 170 K is described by open circles.

Fig. 5. Experimental and calculated weights for Sample 2. For details see the caption of Fig. 3.

Fig. 6. The spectral area of the rigid doublet of Sample 2. The dashed curve represents the contribution of the deuterons of both the hydroxyls, while the solid curve contains also the contribution of CD_3(I). For details see text.

Fig. 7. Experimental relaxation rates and calculated initial rates for the fast, medium and slow components of Sample 3. For details see the caption of Fig. 2.

Fig. 8. Experimental and calculated weights for Sample 3. For details see the caption of Fig. 3.

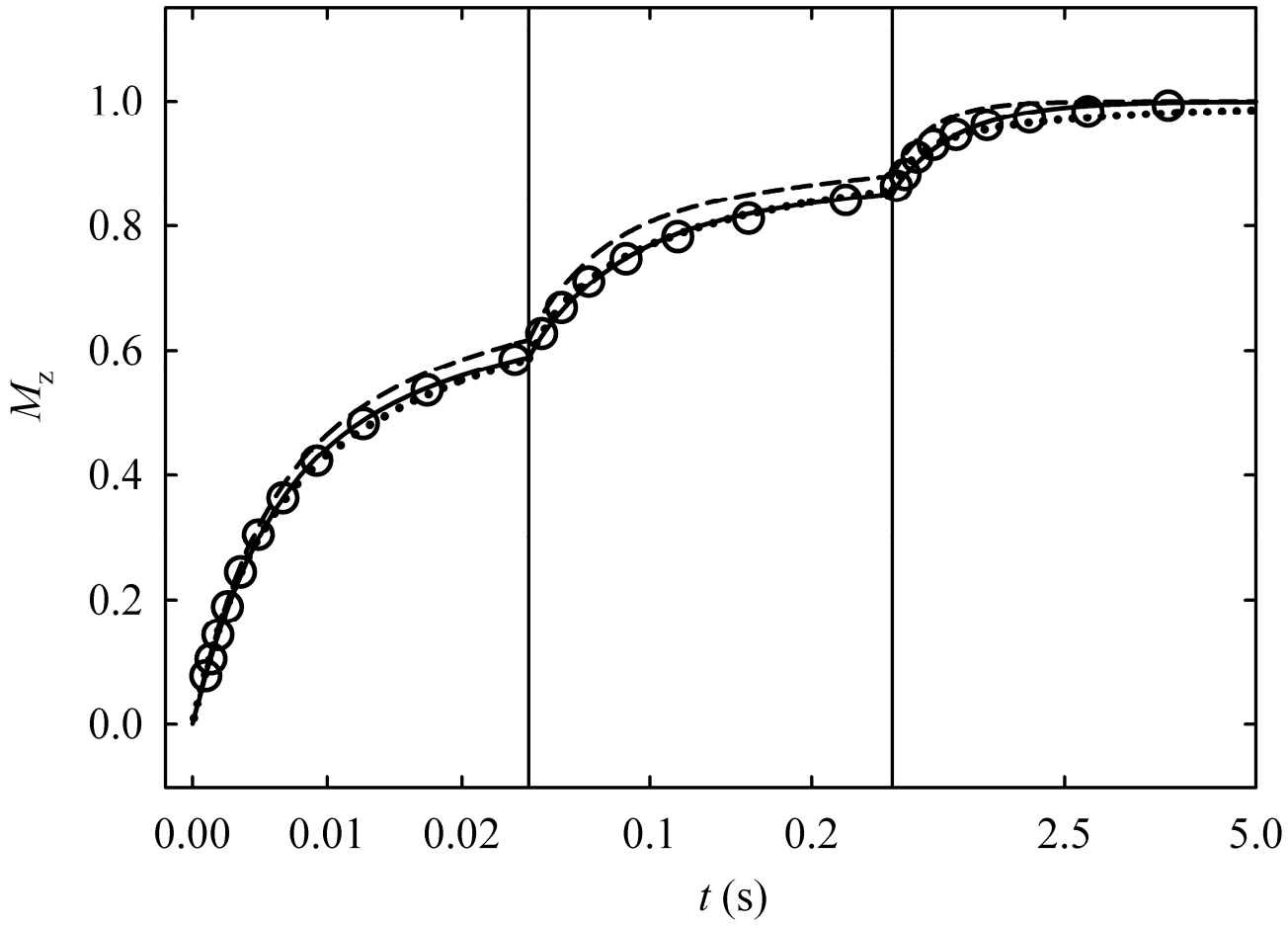

Fig. 1.

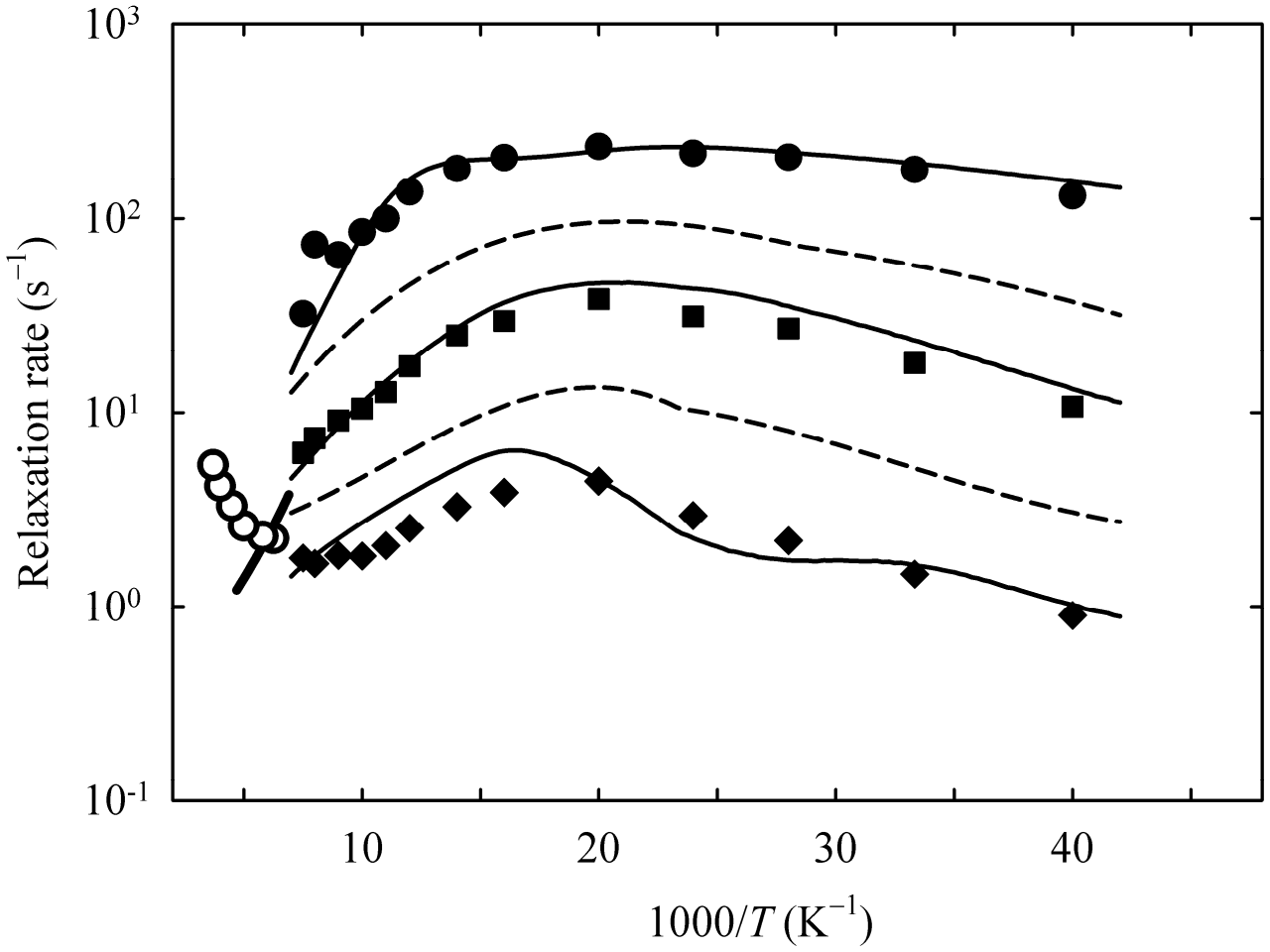

Fig. 2.

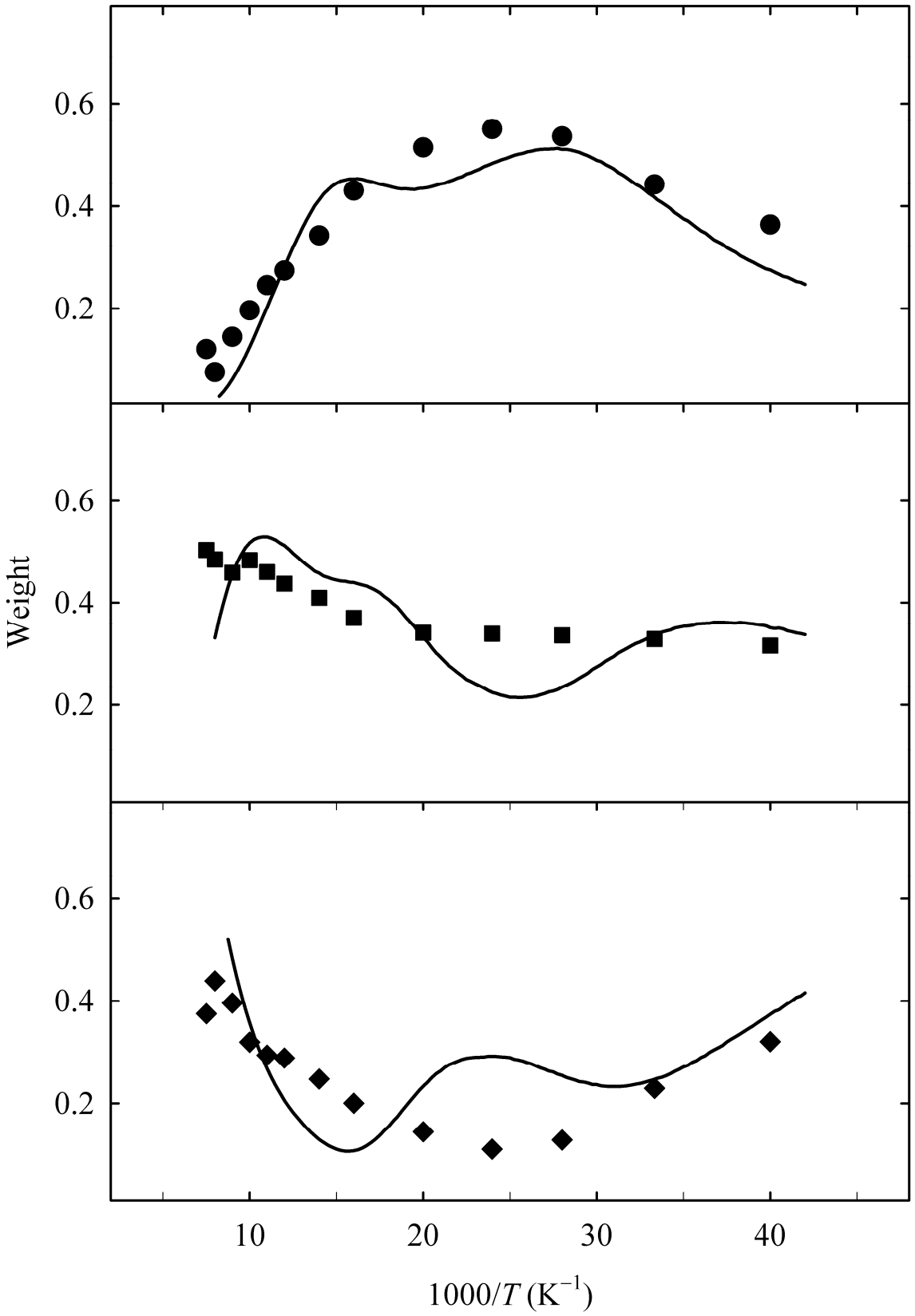

Fig. 3.

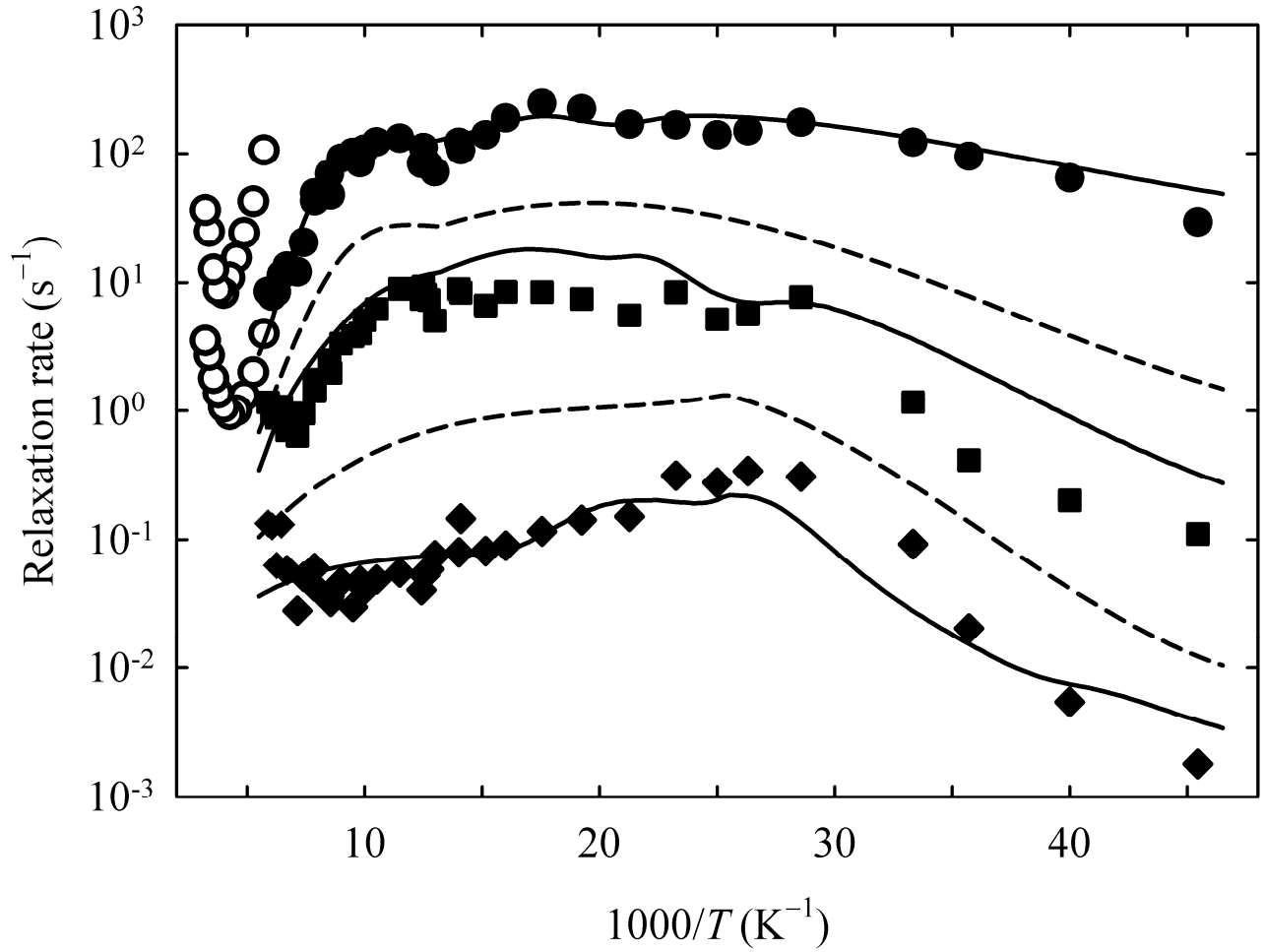
10^3
10^2
10^1
10^0
10^{-1}
10^{-2}
10^{-3}
Relaxation rate (s^{-1})
10
20
30
40
$1000/T$ (K^{-1})

Fig. 4.

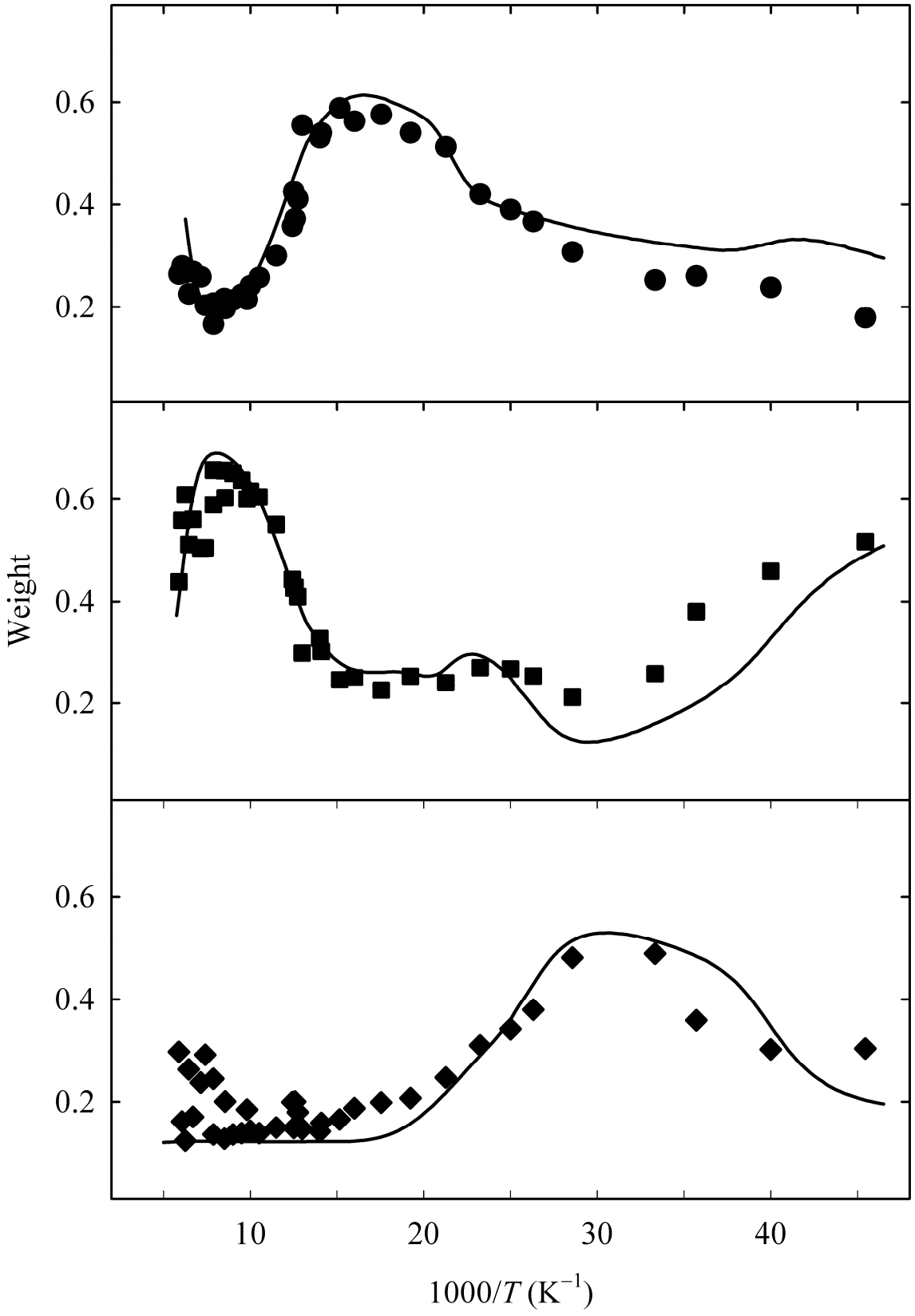

Fig. 5.

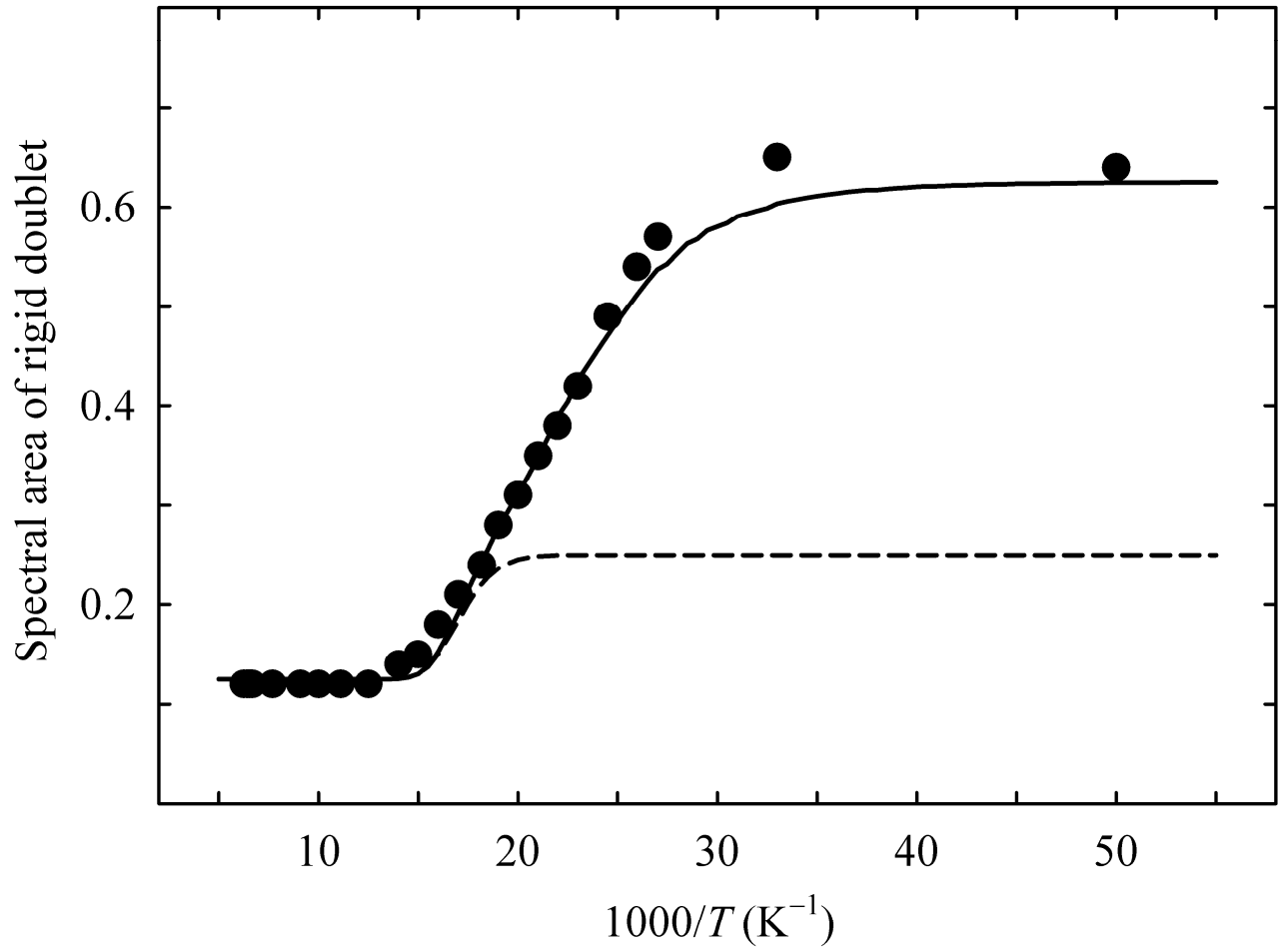

Fig. 6.

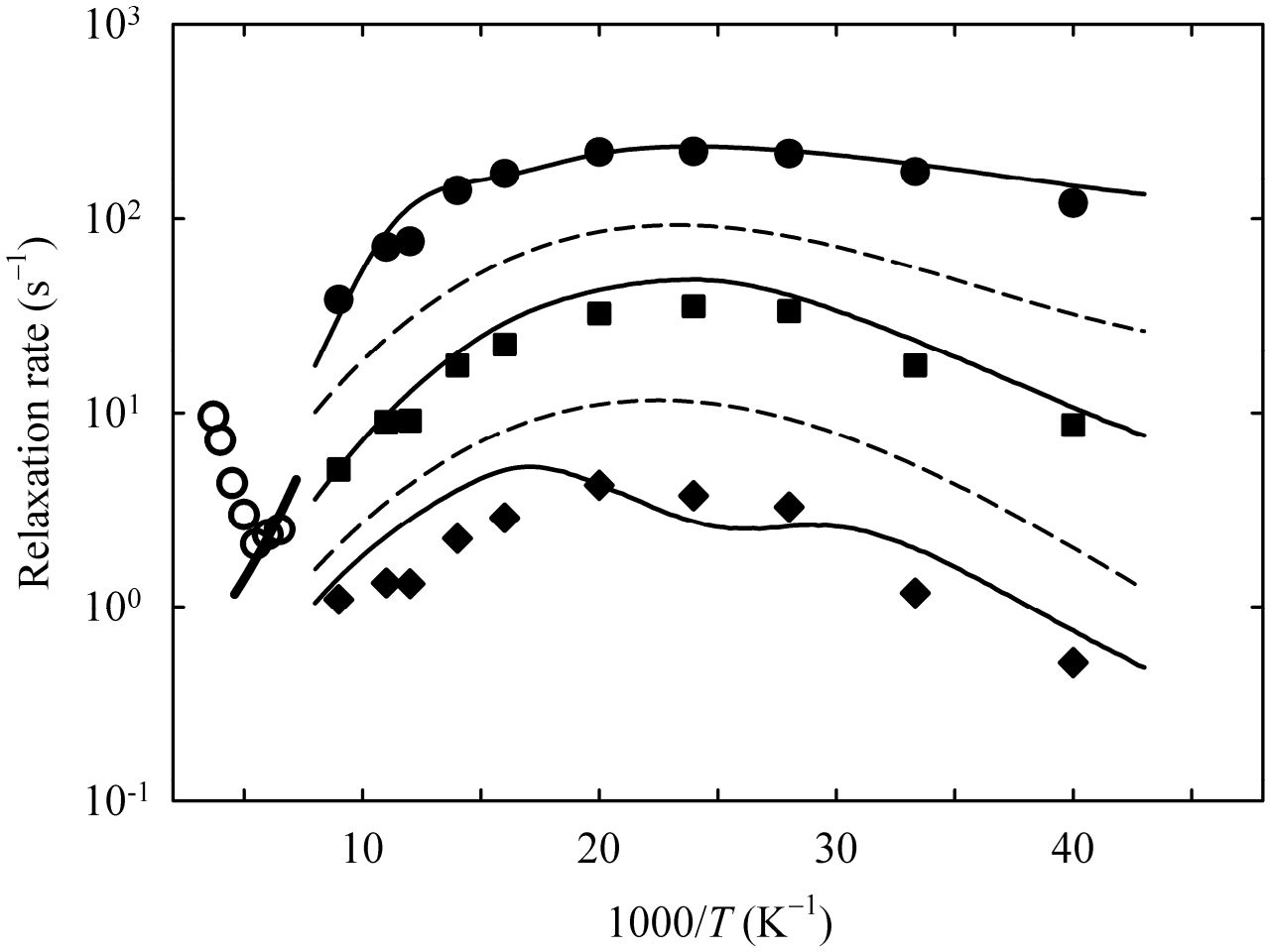

Fig. 7.

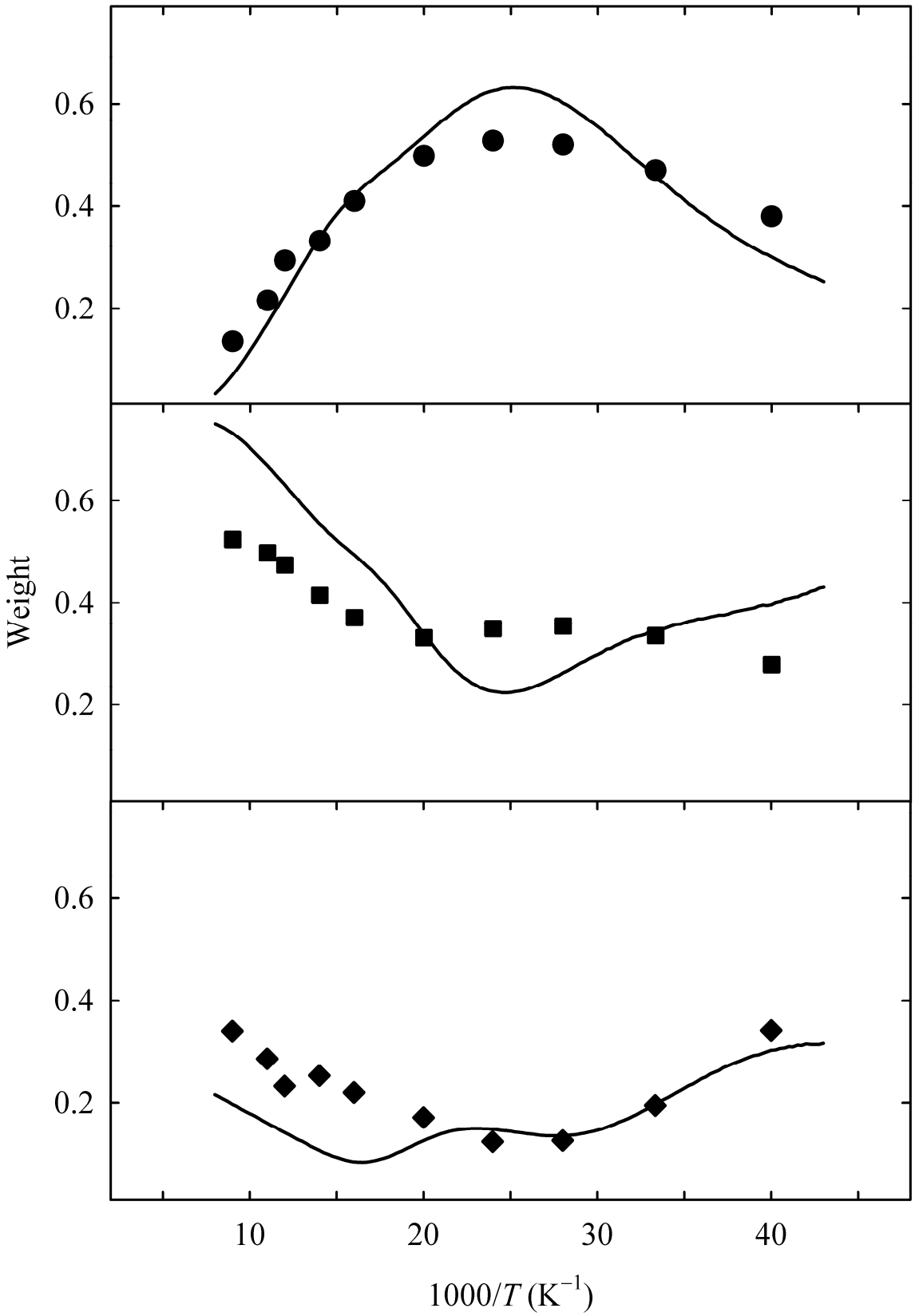

Fig. 8.